Journal of Thermal Analysis and Calorimetry, Vol. 69 (2002) 813–819

CALORIMETRIC AND STRUCTURAL STUDIES OF $La_{1-x}Y_xAlO_3$ AND $Y_{1-x}Lu_xAlO_3$ CRYSTALS

T. Kyomen and M. Itoh[*]

Materials and Structures Laboratory, Tokyo Institute of Technology, 4259 Nagatsuta, Midori-ku, Yokohama 226-8503, Japan

Abstract

Powder X-ray diffraction measurements of $La_{1-x}Y_xAlO_3$ suggested that the space groups of x=0.3 and 0.9 samples are Pnma at room temperature and that a structural phase transition occurs from R-3c to Pnma above 200 K in x=0.1 sample. The unit cell volumes of x=0.1, 0.3, and 0.9 samples at 20 K are larger than the average one estimated from the volumes of $LaAlO_3$ and $YAlO_3$. The heat capacities of x=0.1 and 0.3 samples are larger than those of $LaAlO_3$ in the range 3–20 K. On the other hand, the volumes of $Y_{1-x}Lu_xAlO_3$ (x=0.1, 0.3, and 0.5) at 20 K are close to the average one and the heat capacity increased as x is increased in the range 3–20 K.

Keywords: aluminum lanthanum yttrium oxide, aluminum lutetium yttrium oxide, crystal structure, heat capacity, solid solution

Introduction

Most of perovskite-type oxides, chemical formula of which is written by ABO_3, show useful function such as ferroelectricity, ferromagnetism, fast ion conductivity, and so on. The functional perovskite-type oxides often include plural elements in A and/or B sites, and the plural kinds of atoms are usually arranged in a disordered fashion. In crystals including a certain disorder such as an impurity, it has been reported that a certain low energy excitation mode exists in addition to phonon mode with respect to atomic motions [1–6]. In recent studies of alloy, it has been suggested that an atomic force constant is sensitive to the bond distance [7]. This suggestion implies that ion size is important in the ionic materials.

In the present study, heat capacities of $La_{1-x}Y_xAlO_3$ and $Y_{1-x}Lu_xAlO_3$ were measured in order to clarify the properties of elementary excitations with respect to the atomic motions in the perovskite-type solid-solution systems. The difference in radius of two kinds of A site ion is large and small in the former and the latter systems, respectively [8]. In addition, a phase relation of $LaAlO_3$–$YAlO_3$ solid-solution system was examined by powder X-ray diffraction measurements.

---

[*] Author for correspondence: E-mail: m.itoh@rlem.titech.ac.jp

1418–2874/2002/ $ 5.00

Akadémiai Kiadó, Budapest
Kluwer Academic Publishers, Dordrecht

Experimental

$R_{1-x}R'_xAlO_3$ (*R*, *R*'=La, Y and Y, Lu) polycrystalline samples were prepared from Y_2O_3 (99.99 %), La_2O_3 (99.99 %), Lu_2O_3 (99.9 %), and $Al(NO_3)_3{\cdot}9H_2O$ (98%) by a precursor method using citric acid. $Al(NO_3)_3{\cdot}9H_2O$ was recrystallized once by distilled water and 3–4 mol dm^{-3} aluminum nitrate aqueous solution was prepared. The contents of Al, Y, La, and Lu atoms in the aqueous solution and the starting oxides, respectively, were determined by an EDTA titration. Appropriate amounts of R_2O_3 and R'_2O_3 were dissolved by nitric acid, and then appropriate amounts of aluminum nitrate aqueous solution and citric acid were added. The amount of used citric acid was approximately twice as much as the amount needed to coordinate all metal ions in the solution if all NO_3^- ions were replaced by citric polymer. The solution was dehydrated by heating on a hot plate. As-prepared amorphous precursor was heated up to 1273 K for 6 h in a furnace and calcined there for 12 h. The calcined powder was pressed into a pellet and then sintered at 1673 K for 12 h.

Powder X-ray diffraction (XRD) measurements were carried out for phase analysis at 20, 200, and 300 K. Rietveld analyses of $La_{0.9}Y_{0.1}AlO_3$ and $La_{0.7}Y_{0.3}AlO_3$ were carried out at 300 K by using a RIETAN-2000 program [9]. Lattice constants were determined from XRD peak positions using crystalline silicon powder as an internal standard. Heat capacity measurements were carried out in the temperature range 3–20 K by a relaxation method using a Quantum Design PPMS. The masses of samples used were about 10 mg.

Results

Powder X-ray diffraction measurements

Figure 1 shows powder XRD patterns of $LaAlO_3$, $La_{1-x}Y_xAlO_3$ (x=0.1, 0.3, 0.5, and 0.9), $YAlO_3$, and $Y_{1-x}Lu_xAlO_3$ (x=0.1, 0.3, and 0.5) from the bottom to the top. It has been reported that the space groups of $LaAlO_3$, $YAlO_3$, and $LuAlO_3$ are R-3c (no. 167), Pnma (no. 62), and Pnma, respectively, and that a mixture of $YAlO_3$ and $LuAlO_3$ forms a solid solution with the space group Pnma in all composition range [10, 11]. In the present study, $Y_{1-x}Lu_xAlO_3$ (x=0.1, 0.3, and 0.5) were actually obtained as a single phase and the peak positions were indexed by the space group Pnma. On the other hand, there is no report whether a mixture of $LaAlO_3$ and $YAlO_3$ forms a solid solution or separates to some phases. It was found in the present study that $La_{1-x}Y_xAlO_3$ samples with x=0.1, 0.3, and 0.9 are obtained as a single phase but x=0.5 sample separates to two phases with perovskite-type structure, possibly lanthanum rich and yttrium rich phases.

The space group of $La_{0.1}Y_{0.9}AlO_3$ must be Pnma, because the XRD pattern is similar to those of $YAlO_3$ and all the peak positions are indexed by the space group. Figures 2(a) and 2(b) show powder XRD patterns of $La_{0.9}Y_{0.1}AlO_3$ and $La_{0.7}Y_{0.3}AlO_3$, respectively, in the ranges 2θ=47.8–48.5° and 2θ=108–111° on enlarged scales. Both the diffraction peaks around 48 and 109° do not split in the space group R-3c but split into two peaks in the space group Pnma. The experimental intensities indicated by crosses were thus fitted by assuming one or two diffraction peaks including CuKα_1 and CuKα_2 contributions and a constant base line. The thin and thick solid lines in the figures indicate the respective diffraction peaks and their sum obtained by the fit-

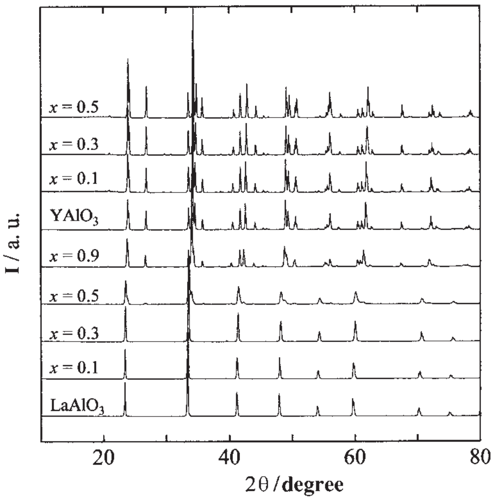

Fig. 1 Powder XRD patterns of $LaAlO_3$, $La_{1-x}Y_xAlO_3$ (x=0.1, 0.3, 0.5, and 0.9), $YAlO_3$, and $Y_{1-x}Lu_xAlO_3$ (x=0.1, 0.3, and 0.5) samples from the bottom to the top. The ordinates are shifted for clarity

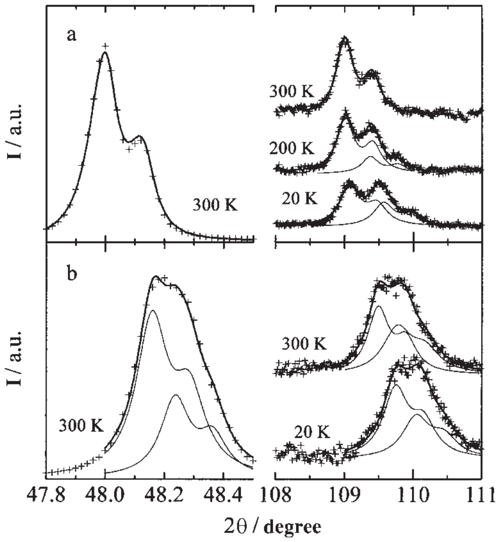

Fig. 2 Powder XRD patterns of a – $La_{0.9}Y_{0.1}AlO_3$ and b – $La_{0.7}Y_{0.3}AlO_3$ samples in the range 2θ=47.8–48.5° and 2θ=108–111° at some temperatures indicated in the figure. The ordinates are shifted for clarity. See text for the lines in the figure

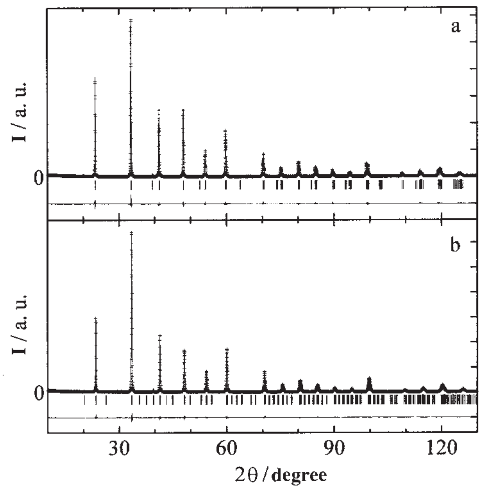

Fig. 3 Results of Rietveld analyses of a – $La_{0.9}Y_{0.1}AlO_3$ and b – $La_{0.7}Y_{0.3}AlO_3$ samples at 300 K assuming the space groups of R-c3 Pnma, respectively: Experimental (crosses) and fitting values (solid line), peak positions (vertical lines), and difference between the experimental and fitting values(solid line) are shown in the upper, middle and lower parts, respectively

tings. The diffraction patterns of $La_{0.7}Y_{0.3}AlO_3$ were well reproduced by assuming two peaks, indicating that the space group is not R-3c both at 20 and 300 K. In $La_{0.9}Y_{0.1}AlO_3$, splitting of peak around 109° is also clear both at 20 and 200 K as seen from a shoulder observed around 110.0 and 109.7°, respectively. On the other hand, splittings of both peaks around 48 and 109° are unclear at 300 K. Therefore, a structural phase transition is expected to take place at least above 200 K in $La_{0.9}Y_{0.1}AlO_3$. (Heat capacity measurements detected no appreciable anomaly due to a phase transition between 200 and 300 K from the possible reasons as follows. The anomaly is small because of the displacive type and broad because of the solid-solution system, the accuracy of measurements is low at such high temperatures, and/or transition temperature is slightly higher than 300 K.) Rietveld analyses of $La_{0.9}Y_{0.1}AlO_3$ and $La_{0.7}Y_{0.3}AlO_3$ were carried out at 300 K by assuming the space groups R-3c and Pnma, respectively. The results are shown in Figs 3(a) and 3(b). Considering that the reliable parameters are sufficiently small, the assumptions of space group are considered to be plausible.

Open and solid circles in Fig. 4(a) represent the compositional dependences of volumes per formula unit of $Y_{1-x}Lu_xAlO_3$ and $La_{1-x}Y_xAlO_3$, respectively. The error bars are smaller than the mark size. The compositional dependence of volume of $La_{1-x}Y_xAlO_3$ seems to deviate from the straight line (solid line in the figure) connecting the volumes of pure materials $LaAlO_3$ and $YAlO_3$. The deviation is largest in x=0.3 sample but exist also both in x=0.1 and 0.9 samples. The compositional dependence of volume of $Y_{1-x}Lu_xAlO_3$ seems to be linear at least in the range x=0–0.5.

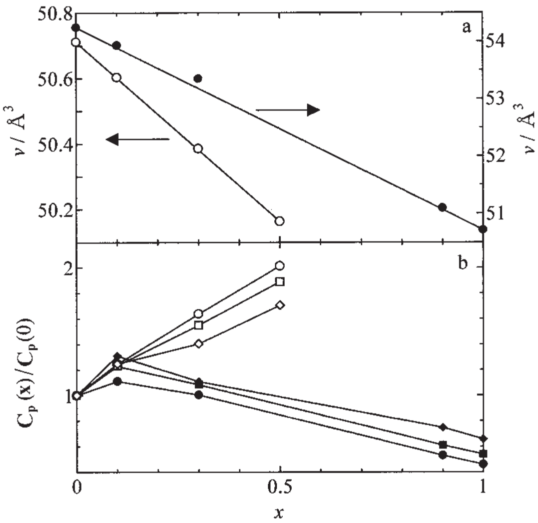

Fig. 4 Compositional dependences of a – volume per formula unit and b – heat capacity. Solid and open symbols are values of $La_{1-x}Y_xAlO_3$ and $Y_{1-x}Lu_xAlO_3$. Circles, squares, and diamonds are values at 20, 15, and 10 K. Solid lines are guide for eyes

Heat capacity measurements

Figures 5(a) and 5(b) show C_p/T *vs.* T^2 plots of $Y_{1-x}Lu_xAlO_3$ (x=0, 0.1, 0.3, and 0.5) and $La_{1-x}Y_xAlO_3$ (x=0, 0.1, 0.3, 0.9, and 1), respectively, in the temperature range 3–20 K. All the curves do not go to the origin, possibly because of the presence of a Schottky anomaly due to small amount of magnetic impurities, judging from the re-

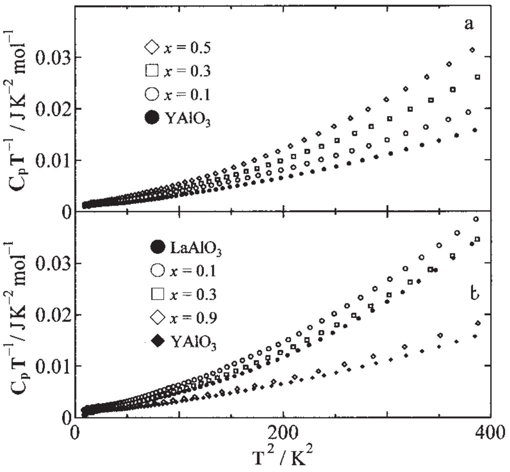

Fig. 5 Plots of heat capacity divided by temperature *vs.* squared temperature: a – $Y_{1-x}Lu_xAlO_3$; b – $La_{1-x}Y_xAlO_3$

sults that the magnitudes of heat capacities were changed by applying 9 T magnetic field particularly below 10 K (not shown). In order to estimate the impurity fraction, the heat capacity data of $LaAlO_3$ and $YAlO_3$ were fitted tentatively by assuming that the heat capacities are a sum of contributions from two-level Schottky anomaly and lattice heat capacity (aT^3+bT^5 term). (Of course, a kind of impurity and the energy level structure are unclear. However, this estimation would give a maximum impurity fraction, because the energy level structure with a number of energy levels more than two results in a larger Schottky anomaly when the ground state has no degeneracy.) The estimated impurity fraction (possibly a maximum value) and energy level splitting were about 0.1% and 12 K, respectively, in both $LaAlO_3$ and $YAlO_3$. The magnetic impurities are likely to come from aluminum nitrate, because the energy level splitting and impurity fraction are nearly same between $LaAlO_3$ and $YAlO_3$ and the other materials, e.g. (La,Y)GaO_3, prepared by the same procedure did not show such a large Schottky anomaly [12]. The contributions to the heat capacity from the Schottky anomaly are at most 5, 1, and 0.2% at 10, 15, and 20 K.

The heat capacities of $La_{0.9}Y_{0.1}AlO_3$ and $La_{0.7}Y_{0.3}AlO_3$ are larger than those of $LaAlO_3$ in the range 3–20 K. In order to clarify the connection between the larger heat capacities and impurities, the same fittings as done in $LaAlO_3$ and $YAlO_3$ were carried out to the data of $La_{0.9}Y_{0.1}AlO_3$ and $La_{0.7}Y_{0.3}AlO_3$ tentatively. The obtained impurity fraction and energy level splitting were about 0.2% and 16 K. Even if the contributions were subtracted from the heat capacity data, the heat capacities of $La_{0.9}Y_{0.1}AlO_3$ and $La_{0.7}Y_{0.3}AlO_3$ are undoubtedly larger than those of $LaAlO_3$ at least above 7 K, indicating no connection between the larger heat capacities and impurities. Figure 4(b) shows compositional dependences of heat capacities divided by the value of $YAlO_3$ or $LaAlO_3$ at 10, 15, and 20 K. The heat capacity ratio of $La_{1-x}Y_xAlO_3$ to $LaAlO_3$ shows a clear maximum around x=0.1. On the other hand, the heat capacity ratio of $Y_{1-x}Lu_xAlO_3$ to $YAlO_3$ increases as x is increased but seems to have a shoulder around x=0.1. However, it is unclear whether the shoulder is connected with the impurities or not, because excess heat capacities due to the shoulder is small even at 10 K.

Discussion

It was found that heat capacities of $La_{0.9}Y_{0.1}AlO_3$ and $La_{0.7}Y_{0.3}AlO_3$ were larger than those of $LaAlO_3$ in the range 3–20 K in spite of the smaller formula mass and volume. Contribution to the larger heat capacities from phonon softening due to R-3c to Pnma phase transition would be so small (if any) below 20 K because the transition temperature is rather high (above 200 K even in $La_{0.9}Y_{0.1}AlO_3$). One may consider that the difference in the space group between Pnma and R-3c is reason for the larger heat capacities in $La_{0.9}Y_{0.1}AlO_3$ and $La_{0.7}Y_{0.3}AlO_3$. However, if the high-temperature R-3c phase were realized at low temperatures, the heat capacity of R-3c phase is likely to be larger than those of low-temperature Pnma phase at the same temperature, because the entropy of low-temperature phase is usually smaller than that of supercooled high-temperature phase. Therefore, the larger heat capacities of $La_{0.9}Y_{0.1}AlO_3$ and $La_{0.7}Y_{0.3}AlO_3$ are unlikely to connect with the difference in the space group. The excitation energy (frequency) with respect to atomic motions is associated with the mass of constituent atoms and the atomic force constants. As a mass is increased or an atomic force constant is decreased, the excitation energy decreases and thus the heat capacity increases. The larger heat capacities of $La_{0.9}Y_{0.1}AlO_3$ and $La_{0.7}Y_{0.3}AlO_3$ are likely to originate from some decreased atomic force constants as compared to those of $LaAlO_3$, because the average mass of A site ions (formula weight) decreases linearly as x is increased. The larger unit cell volume of $La_{0.9}Y_{0.1}AlO_3$ and $La_{0.7}Y_{0.3}AlO_3$ than the average volume of pure materials $LaAlO_3$ and $YAlO_3$ might be also associated with the decreased atomic force constant in the solid-solution system.

Concluding remarks

The volumes of $La_{1-x}Y_xAlO_3$ (x=0.1, 0.3, and 0.9) at 20 K are larger than the average one calculated from the values of pure materials $LaAlO_3$ and $YAlO_3$. In addition, the heat capacities of $La_{0.9}Y_{0.1}AlO_3$ and $La_{0.7}Y_{0.3}AlO_3$ are larger than those of $LaAlO_3$ in the range 3–20 K. On the other hand, such the behaviors were not observed both in the volume and heat capacity of $Y_{1-x}Lu_xAlO_3$. By the way, in an AB alloy, a solid solution is thermodynamically stable at low temperatures if A–B interaction is stronger than the average of A–A and B–B interactions, on the other hand, phase separation to A rich and B rich phases is thermodynamically stable at low temperatures if A–B interaction is weaker than the average of A–A and B–B interactions. Therefore, the difference between $La_{1-x}Y_xAlO_3$ and $Y_{1-x}Lu_xAlO_3$ systems might be associated with the facts that $Y_{1-x}Lu_xAlO_3$ is a solid-solution system in the whole composition range [11], on the other hand, $La_{1-x}Y_xAlO_3$ is essentially a phase-separation system as found from the result that x=0.5 sample is separated to two phases.

References

1 J. P. Harrison, P. P. Peressini and R. O. Pohl, Phys. Rev., 171 (1968) 1037.
2 W. N. Lawless, Phys. Rev. B, 21 (1980) 585.
3 D. G. Cahill and R. O. Pohl, Phys. Rev. B, 39 (1989) 10477.
4 K. A. Topp and D. G. Cahill, Z. Phys. B, 101 (1996) 235.
5 H. E. Fischer, F. J. Bermejo, G. J. Cuello, M. T. Fernandez-Diaz, J. Dabrowski, M. Jimenez-Ruiz and H. Schober, Europhys. Lett., 46 (1999) 643.
6 T. Tojo, T. Atake, T. Mori and H. Yamamura, J. Chem. Thermodyn., 31 (1999) 831.
7 A. van de Walle and G. Ceder, Rev. Mod. Phys., 74 (2002) 11.
8 R. D. Shannon, Acta Crystallogr. A, 32 (1976) 751.
9 F. Izumi and T. Ikeda, Mater. Sci. Forum, 321-324 (2000) 198.
10 T. Shishido, S. Nojima, M. Tanaka, H. Horiuchi and T. Fukuda, J. Alloy and Compounds, 227 (1995) 175.
11 A. G. Petrosyan, G. O. Shirinyan, K. L. Ovanesyan, C. Pedrini and C. Dujardin, J. Cryst. Growth, 198/199 (1999) 492.
12 T. Kyomen et al., unpublished.